

Spatially selective Bragg scattering: a signature for vortices in Bose-Einstein condensates.

P. B. Blakie¹ and R. J. Ballagh^{1,2}

¹*Department of Physics, University of Otago, P. O. Box 56, Dunedin, New Zealand*

²*Institute for Theoretical Physics, University of Innsbruck, A-6020 Innsbruck, Austria*

(November 1, 2018)

We demonstrate that Bragg scattering from a condensate can be sensitive to the spatial phase distribution of the initial state. This allows preferential scattering from a selected spatial region, and provides a robust signature for a vortex state. We develop an analytic model which accurately describes this phenomenon and we give quantitative predictions for current experimental conditions.

PACS numbers: 05.30.Jp, 03.75.Fi

Bragg scattering of matter waves from laser beams is a well known phenomenon in atom optics [e.g. [1,2]] and has proved to be an effective tool for manipulating and analysing Bose condensates. In that context it has been used in experiments to coherently split a condensate [3,4], and to perform momentum and phonon spectroscopy [5,6]. Theoretical calculations show it may be used to extract quasiparticle amplitudes from weakly excited condensates [7]. Two groups have constructed Mach-Zehnder type interferometers [8] using sequences of Bragg pulses to probe condensate phase [9–11]. In all of those cases the Bragg scattering process is most easily understood in terms of a momentum space process in which the Bragg fields transfer momentum $\hbar\mathbf{q}$ to each atom. In a beam-splitter, half the initial amplitude is translated in momentum space by $\hbar\mathbf{q}$, while in momentum spectroscopy a selected narrow group of momentum components is translated by $\hbar\mathbf{q}$. The spatial structure of the initial condensate plays no particular role in the Bragg process for those cases.

A major interest in condensates however, is that their macroscopic wavefunctions may be engineered into specific spatial structures. For example, the vortex state, which has been recently observed by two groups [12,13], has a phase circulation of 2π about a vortex core. The most direct means for observing such a phase distribution is by interference with a separate well characterised matter field [e.g. [14,12]], but this may not always be experimentally convenient. In this paper we show that under appropriate conditions Bragg scattering is sensitive to the spatial phase distribution of the initial condensate and therefore allows preferential scattering from a selected spatial region. In the case of a vortex, this gives a distinctive signature which we illustrate in Fig. 1. There the density distribution of a trapped condensate vortex state is shown following application of Bragg pulse chosen according to criteria developed later in this paper. In Fig. 1(a) the streaming output emerges from only one side of the initial condensate, and gives an asymmetric density pattern which should be detectable with current experimental technology. In Fig. 1(b) where the

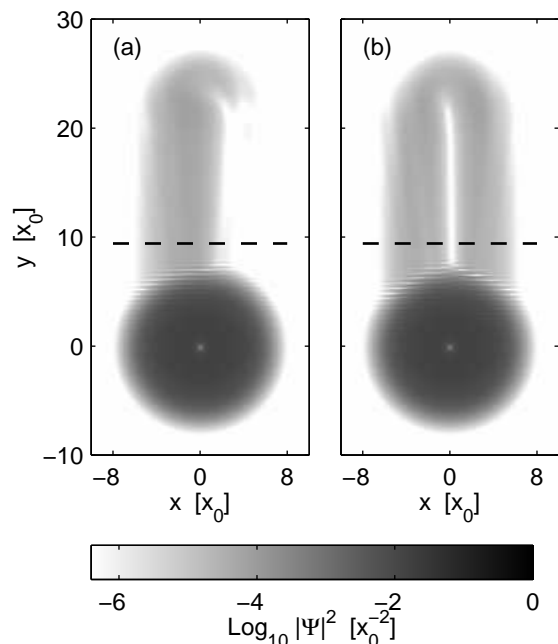


FIG. 1. Spatial density of a 2D vortex state at time $t = 0.6t_0$ after excitation by a Bragg pulse with frequency detuning (a) $\omega = 216\omega_T$ and (b) $\omega = 203\omega_T$ (ω_T is the harmonic trapping frequency). Other parameters are $V = 0.2\omega_T$, $q = 14/x_0$ and $w = 500w_0$. Units: time $t_0 = 1/\omega_T$; distance $x_0 = \sqrt{\hbar/2m\omega_T}$; collisional interaction strength $w_0 = \hbar\omega_T x_0^3$. The dashed line denotes a suitable position for measuring the output beam profile (see text).

frequency difference of the laser fields has been changed, the streaming output field has a density node that is an order of magnitude wider than the vortex core itself (i.e. the healing length in the centre of the original condensate). In the following we develop a treatment of such *spatially selective Bragg scattering* which explains the behaviour in terms of the underlying spatial phase sensitive mechanism and we give analytic solutions appropriate to 3D condensates. We treat the process of Bragg scattering from a condensate using a previously developed

formalism [15], in which the condensate mean-field Ψ (in an interaction picture) evolves in a far detuned light-field grating formed by two plane-wave laser beams, according to the equation

$$i\hbar\frac{\partial}{\partial t}\Psi = \left[-\frac{\hbar^2}{2m}\nabla^2 + V_T(\mathbf{r}) + w|\Psi|^2 \right] \Psi + \hbar V(t) \cos(\mathbf{q} \cdot \mathbf{r} - \omega t) \Psi. \quad (1)$$

Here $V_T(\mathbf{r})$ is the trap potential (assumed to be harmonic in the examples of this paper) and w ($= 4N\pi\hbar^2 a/m$) is the usual nonlinearity parameter of the Gross-Pitaevskii equation. The final term in Eq. (1) describes the interaction with the Bragg grating: ω and $\hbar\mathbf{q}$ are the two-photon detuning and recoil momentum respectively and $V(t) = |\Omega(t)|^2/2\Delta$ is twice the ac-stark shift at the intensity peaks. For the scattering to be in the Bragg regime the pulse length T_p of the lasers must be long enough that the Bragg resonance is resolved (i.e. $T_p \gg \omega_q^{-1}$, where $\omega_q = \hbar q^2/2m$ is the recoil frequency). In order to obtain *spatially selective Bragg scattering* it is also necessary that the average value of V is sufficiently small that the total amount of condensate scattered in time T_p is small compared to the unscattered amount. In addition we assume the Bragg pulse length (and the time of observation) is shorter than a quarter trap period, to avoid the trap forces significantly altering the momentum of the scattered beam.

Equation (1) can be directly numerically simulated, as for example we have shown in the two dimensional case of Fig. 1. We have also obtained an analytic solution, which provides detailed insight into the underlying physics and enables us to provide quantitative calculations over a wide range of parameters in the three dimensional case. For the analytic solution, we assume that the recoil momentum $\hbar\mathbf{q}$ of the Bragg grating is much larger than the momentum width of the initial condensate (which is centred about zero momentum), and also assume that the detuning ω is close to the Bragg resonance. This means the scattered wavepacket is well separated in momentum space from the initial state and a slowly varying envelope approximation can be made [16] so that we write

$$\Psi(\mathbf{r}, t) = \psi_0(\mathbf{r}, t) + \psi_1(\mathbf{r}, t) e^{i(\mathbf{q} \cdot \mathbf{r} - \omega t)}. \quad (2)$$

In Eq. (2) ψ_1 is the scattered wavepacket while ψ_0 , which we call the mother condensate, represents a condensate with a momentum wavepacket centered on zero. At $t = 0$, ψ_0 is exactly the initial condensate. Substituting Eq. (2) into Eq. (1) and projecting into orthogonal regions of momentum space, we obtain to first order in ψ_1 the coupled equations

$$i\hbar\frac{\partial}{\partial t}\psi_0 = \left[-\frac{\hbar^2}{2m}\nabla^2 + V_T + w|\psi_0|^2 \right] \psi_0 + \frac{\hbar V(t)}{2} \psi_1, \quad (3)$$

$$i\hbar\frac{\partial}{\partial t}\psi_1 = \left[-\frac{\hbar^2}{2m}\nabla^2 - \hbar\delta - i\hbar\mathbf{Q} \cdot \nabla + V_T \right. \quad (4)$$

$$\left. + 2w|\psi_0|^2 \right] \psi_1 + \frac{\hbar V(t)}{2} \psi_0,$$

where $\mathbf{Q} = \hbar\mathbf{q}/m$ is the velocity of the scattered atoms, $\delta = \omega - \omega_q$ and we have neglected the rapidly oscillating term $\psi_0^2\psi_1^*$. Our interest is in the scattered state ψ_1 which is assumed to be small, so we can neglect the scattering from ψ_1 back to ψ_0 (i.e. $V(t)\psi_1$ in Eq. (3)). This means that ψ_0 then evolves according to the usual Gross-Pitaevskii equation, and typically we choose ψ_0 to be an eigenstate of that equation. We can also ignore the ∇^2 term in Eq. (4) which describes momentum diffusion about the centre of momentum \mathbf{q} of the ψ_1 packet, and is small on the time scales we consider. Eq. (4) can now be solved to give

$$\psi_1(\mathbf{r}, t) = -\frac{i}{2} \int ds e^{-iK(\mathbf{r}, t, s)} V(s) \psi_0(\mathbf{r} + \mathbf{Q}(s-t), s), \quad (5)$$

where

$$K(\mathbf{r}, t, s) = (s-t)\delta + \frac{1}{\hbar} \int_s^t ds' \left[V_T(\mathbf{r} + \mathbf{Q}(s'-t)) + 2w|\psi_0(\mathbf{r} + \mathbf{Q}(s'-t), s')|^2 \right]. \quad (6)$$

Eq. (5) allows us to visualise the formation of the scattered state as follows. As the scattered packet moves across the mother condensate, the amplitude ψ_1 at a given point (stationary in the frame moving with velocity \mathbf{Q}) is built up from the sum of contributions coupled in from successive points along the mother condensate. The contribution coupled in at time s from a position $\mathbf{r} + \mathbf{Q}(s-t)$ on the mother condensate evolves to time t with the propagator $\exp(-iK(\mathbf{r}, t, s))$. The scattered state at \mathbf{r} and t will be appreciable only if the contributions constructively interfere. Writing $\psi_0(\mathbf{r}, s)$ in terms of amplitude and phase $A_0(\mathbf{r}, s) \exp(iS_0(\mathbf{r}, s))$, then the condition for an appreciable scattered state to form is that the phase $\Theta(\mathbf{r}, t, s) = -K(\mathbf{r}, t, s) + S_0(\mathbf{r} + \mathbf{Q}(s-t))$ be stationary. We take ψ_0 to be a stationary eigenstate, i.e. $\psi_0(\mathbf{r}, s) = A_0(\mathbf{r}) \exp(i(S_0(\mathbf{r}) - \mu_0 s))$, where μ_0 is the eigenvalue of the mother condensate. Furthermore we make use of the Thomas Fermi solution $w[A_0]^2 = \mu_0 + V_T$ so then

$$K \approx (t-s)(\mu_0 - \delta) + \frac{w}{\hbar} \int_s^t ds' [A_0(\mathbf{r} + \mathbf{Q}(s'-t))]^2. \quad (7)$$

The condition for stationary phase $d\Theta(\mathbf{r}, t, s)/ds = 0$ then gives the *generalised Bragg resonance condition*

$$\delta \approx \left[\frac{w}{\hbar} [A_0(\mathbf{R})]^2 + \nabla_{\mathbf{R}} S_0(\mathbf{R}) \cdot \mathbf{Q} \right]_{\mathbf{R}=\mathbf{r}+\mathbf{Q}(s-t)}. \quad (8)$$

If Θ has sufficiently large spatial curvature, one particular time s may dominate the stationary phase contribution. However for the cases of a ground or vortex initial

state, Θ varies sufficiently slowly that most contributions from along the line $\mathbf{R} = \mathbf{r} + \mathbf{Q}(s - t)$ on the initial condensate can be in phase. For an initial ground state, Eq. (8) reduces in the linear case to the usual Bragg resonance condition $\delta = 0$, while for the nonlinear case, $\delta = \{w|\psi_0(\mathbf{R})|^2/\hbar\}$ in which the braces indicate that the precise value of the shift is obtained by a suitable average along the path \mathbf{R} [17]. For a general initial state the second term in Eq. (8), which can be interpreted as a Doppler condition, must be included.

The full spatial solution for the scattered state contains a great deal of information, but we can extract a useful and compact signature by considering the steady-state density profile of the scattered beam at the edge of the initial condensate. In the 2D simulation of Fig. 1 for example, the steady-state density profile could be measured along the dashed line. For definiteness, we shall take the case where \mathbf{q} is in the y direction. We define the steady-state density profile of the scattered state to be

$$\mathcal{D}_q(x, z, \omega) = |\psi_1(x, y = R, z, \tau_S)|^2, \quad (9)$$

where the distance R is sufficiently large that the density of the mother condensate in the plane $(x, y = R, z)$ is negligible (i.e. $\mathcal{D}_q \approx |\Psi|^2$). For strongly interacting condensates it is suitable to use $R = R_{TF}$, where R_{TF} is the Thomas-Fermi radius (in the xy -plane). τ_S , the time to reach steady state can be estimated as $2R/Q$, i.e. the time for the scattered state to traverse the mother condensate. Since experiments would usually measure the density projected along the z axis (the line of viewing), we define the projected *steady-state density profile*

$$D_q(x, \omega) = \int dz \mathcal{D}_q(x, z, \omega), \quad (10)$$

to characterise the results of the Bragg scattering.

We begin by considering the case of two spatial dimensions, which contains the essence of the physics. Fig. 2 shows $D_q(x, \omega)$ calculated from the full 2D numerical solution of Eq. (1), for cases where the initial state is (a) a noninteracting ground state (b) a condensate ground state, (c) a condensate vortex state. In Fig. 2 (d)-(f) we provide the comparison to the analytic solutions for the same cases, and it is apparent that agreement is very good. We note that in the analytic solutions a Thomas Fermi approximation is made for ψ_0 . For vortex states, the additional centrifugal potential $m^2/(x^2 + y^2)$ is included and the phase is $S_0(\mathbf{r}) = m \arctan(y/x)$.

The results for the noninteracting ground state (Fig. 2(a) or (d)) show, as expected, that the scattered beam is greatest (i.e. Bragg scattering is resonant) when $\omega = \omega_q$ (i.e. $\delta = 0$). The frequency width of $D_q(x, \omega)$ can be estimated using a simple Fourier analysis on the integral in Eq. (5), to be $\Delta_D \sim Q/R_{TF}$. In Fig. 2(b) [or (e)] the effects of the condensate nonlinearity appear. At the centre of the scattered profile ($x = 0$) the resonant frequency for

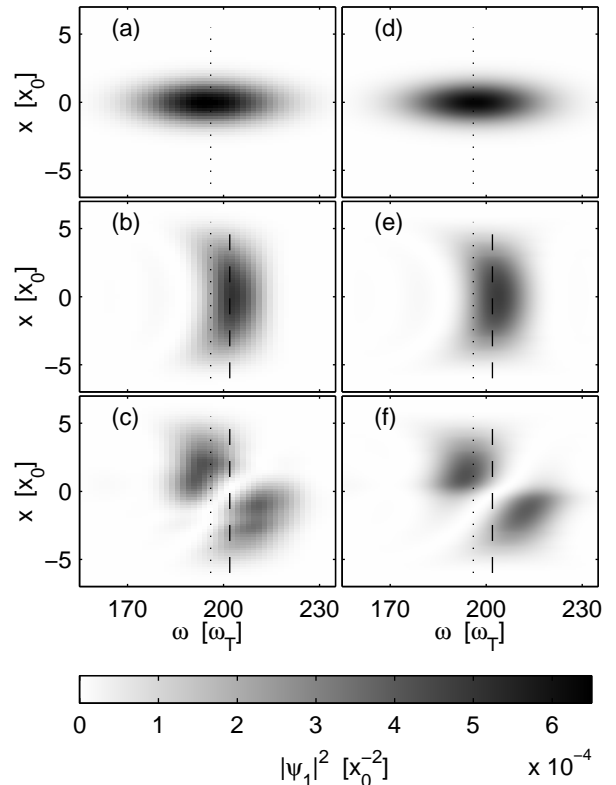


FIG. 2. Steady-state Bragg scattered density profiles in 2D for (a) noninteracting ground state [18], (b) condensate ground state ($w = 500w_0$), (c) condensate vortex state ($w = 500w_0$, $m = -1$). Measurements are made at $t = 0.6t_0$ for a Bragg field with $V = 1\omega_T$, $q = 14/x_0$. Frames (d)-(f) give the analytic solution of Eq. (5) for the cases corresponding to (a)-(c) respectively. Dotted lines, free particle resonant frequency ($\omega_q = \hbar q^2/2m$); dashed lines, 2D nonlinear shifted frequency ($\omega_{nl} = \omega_q + 2\mu_0/3$) [17].

Bragg scattering has been shifted by $.84\mu$ which is close to the value of $\{w|\psi_0(\mathbf{R})|^2/\hbar\}$ averaged along the centre line of the mother condensate ($=4\mu_0/5$). The shift at the spatial edges of the scattered beam ($x = \pm R_{TF}$) is less, because the mother condensate has lower average density along the appropriate lines $\mathbf{R} = \mathbf{r} + \mathbf{Q}(s - t)$, and so $D_q(x, \omega)$ has a crescent shape. The frequency width Δ_D (at $x = 0$) is smaller than for the noninteracting ground state case (a), due mainly to the increased spatial width R_{TF} of the mother condensate. The most significant result for this paper is Fig. 2(c), namely the vortex signature. At the ‘resonant’ frequency (indicated by the dashed line), the scattered density profile is essentially spatially symmetric (see also Fig. 1(b)), but at other frequencies the scattering is spatially asymmetric. This asymmetry, which we emphasize arises from the spatial phase asymmetry of the vortex, is robust, being present for a wide range of frequencies. The density node at the centre of the beam ($x = 0$) at the resonant frequency

also arises from the phase asymmetry: as the scattered wavepacket passes over the vortex core, the contributions from the mother condensate change phase sharply by π and thus cancel. Our results can also be extended into

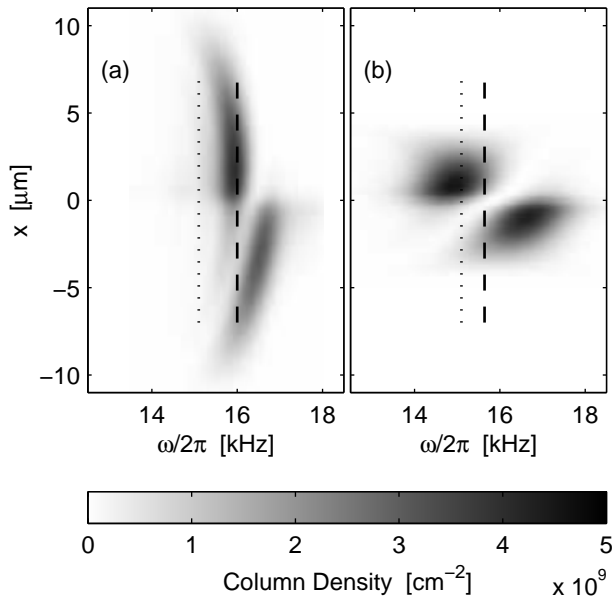


FIG. 3. Projected steady-state Bragg scattered density profiles from a condensate of 2×10^5 Rb⁸⁷ atoms in an $m = -1$ central vortex in (a) prolate trap with $\omega_T = 2\pi \times 50\text{Hz}$, aspect ratio $\lambda = \sqrt{8}$, $\mu_0 \approx 31.6\omega_T$; (b) oblate trap with $\omega_T = 2\pi \times 100\text{Hz}$, $\lambda = 1/10$, $\mu_0 \approx 9.5\omega_T$. Dotted lines, free particle resonant frequency ($\omega_q = 2\pi \times 15\text{kHz}$); dashed lines, 3D nonlinear shifted frequency ($\omega_{nl} = \omega_q + 4\mu_0/7$). Bragg field ($V = 2\pi \times 50\text{Hz}$) provided by counter-propagating lasers of approximately 780nm .

three dimensions by using the analytic solution Eq. (5). In Fig. 3 we present the behaviour of $D_q(x, \omega)$ from a vortex condensate of 2×10^5 Rubidium atoms in both oblate and prolate traps. The features discussed in the previous paragraphs are unchanged in three dimensions. It is worth noting that our results can be readily connected to the well known dynamic structure factor $S(\mathbf{q}, \omega)$ which has been previously used to characterise the results of Bragg scattering [5,6,19]. One can show, within perturbation theory, that

$$S(\mathbf{q}, \omega) \sim \int dx D_q(x, \omega). \quad (11)$$

In other words, the dynamic structure factor simply projects out all the spatial information of the steady-state density profile.

Although we have concentrated on the steady state density profile our analytic solution contains other interesting results. For example, with a Bragg pulse of length $T_p \ll \tau_s$, the scattered state is itself a vortex, and a

sequence of such pulses would produce a sequence of vortices streaming out from the mother condensate, until it becomes too depleted.

In summary we have shown that under appropriate conditions Bragg scattering is sensitive to the spatial phase dependence of the initial matter field state, and therefore allows preferential scattering from a selected spatial region. We have developed an analytic model which accurately describes this phenomenon and explains the underlying mechanisms. When applied to a vortex state, a robust signature is obtained, for both oblate and prolate traps.

This research was supported by the Marsden Fund of New Zealand under contract PVT902. RJB is grateful for the hospitality of the Institute for Theoretical Physics, University of Innsbruck, where part of this research was carried out, and for the support of the Austrian Science Foundation.

-
- [1] P. J. Martin, B. G. Oldaker, A. H. Miklich, and D. E. Pritchard, *Phys. Rev. Lett.* **60**, 515 (1988).
 - [2] P. R. Berman, *Atom Interferometry*, (Academic Press, London, 1997).
 - [3] M. Kozuma, L. Deng, E. W. Hagley, J. Wen, R. Lutwak, K. Helmerson, S. L. Rolston, and W. D. Phillips, *Phys. Rev. Lett.* **81**, 871 (1999).
 - [4] L. Deng, E. W. Hagley, J. Wen, M. Trippenbach, Y. Band, P. S. Julienne, J. E. Simsarian, K. Helmerson, S. L. Rolston, and W. D. Phillips, *Nature* **398**, 218 (1999).
 - [5] J. Stenger, S. Inouye, A. P. Chikkatur, D. M. Stamper-Kurn, D. E. Pritchard, and W. Ketterle, *Phys. Rev. Lett.* **82**, 4569 (1999).
 - [6] D. M. Stamper-Kurn, A. P. Chikkatur, A. Görlitz, S. Inouye, S. Gupta, D. E. Pritchard, and W. Ketterle, *Phys. Rev. Lett.* **83**, 2876 (1999).
 - [7] A. Brunello, F. Dalfovo, L. Pitaevskii, and S. Stringari, *Phys. Rev. Lett.* **85**, 4422 (2000).
 - [8] Y. Torii, Y. Suzuki, M. Kozuma, T. Sugiura, T. Kuga, L. Deng, and E. W. Hagley, *Phys. Rev. A*, **61**, 041602(R) (2000).
 - [9] M. Kozuma, Y. Suzuki, Y. Torii, T. Sugiura, T. Kuga, E. W. Hagley, and L. Deng, *Science* **286**, 2309 (1999).
 - [10] J. E. Simsarian, J. Denschlag, M. Edwards, C. W. Clark, L. Deng, E. W. Hagley, K. Helmerson, S. L. Rolston, and W. D. Phillips, *Phys. Rev. Lett.* **85**, 2040 (2000).
 - [11] J. Denschlag, J. E. Simsarian, D. L. Feder, C. W. Clark, L. A. Collins, J. Cubizolles, L. Deng, E. W. Hagley, K. Helmerson, W. P. Reinhardt, S. L. Rolston, B. I. Schneider, and W. D. Phillips, *Science* **287**, 97 (2000).
 - [12] M. R. Matthews, B. P. Anderson, P. C. Haljan, D. S. Hall, C. E. Wieman, and E. A. Cornell, *Phys. Rev. Lett.* **83**, 2498 (1999).
 - [13] K. W. Madison, F. Chevy, W. Wohlleben, and J. Dalibard, *Phys. Rev. Lett.* **84**, 806 (2000).

- [14] E. L. Bolda and D. F. Walls, Phys. Rev. Lett. **81**, 5477 (1998).
- [15] P. B. Blakie and R. J. Ballagh, J. Phys. B **33**, 3961 (2000).
- [16] M. Trippenbach, Y. B. Band, and P. S. Julienne, Phys. Rev. A **62**, 023608 (2000).
- [17] This shift, suitably averaged over all paths through the condensate corresponds to the shift measured in [5,6]. The Thomas Fermi values for 2D and 3D are $2\mu_0/3$ and $4\mu_0/7$ respectively (see [5]).
- [18] For the case $w = 0$ we use a gaussian wavefunction for ψ_0 , with $\mu_0 = 0$.
- [19] F. Zambelli, L. Pitaevskii, D. M. Stamper-Kurn, and S. Stringari, Phys. Rev. A **61**, 063608 (2000).